



Inhibition Efficiency of Erdosteine Drug for 304L Stainless Steel Corrosion and Its Solvation Thermodynamic Parameters



Abd El-Aziz S. Foudaa, Farid I. El-Dossoki b*, Eladl A. Hamed b, Ahmed El-Hossiany a,b

^a Department of Chemistry, Faculty of Science, El-Mansoura University,

^b Department of Chemistry, Faculty of Science, Port Said University, Port Said, 42526 Egypt

^c Delta for Fertilizers and Chemical Industries, Talkha, Daqahlya 1179 Egypt

Abstract

The effect of a new class of corrosion inhibitor, namely, Erdosteine drug on stainless steel 304L (304L SS) corrosion was investigated as potential corrosion inhibitor in 1 M HCl solution at 25°C. Measurements were conducted utilizing “weight loss (WL), electrochemical impedance spectroscopy (EIS) and potentiodynamic polarization (PP)” tests. From all tests, one can observe that with increasing doses of Erdosteine drug the inhibition efficacy was increased at 25°C. The adsorption of this drug on SS304L surface follows Langmuir adsorption isotherm. The inhibition efficacy increases with increasing the dose of the Erdosteine drug and decreases with rise in temperature of the medium. This drug may form a film which acts as a barrier, to minimize the contact area between 304L SS surface and HCl solution. Electrochemical results showed that this drug is efficient inhibitor for SS304L and the efficacy reached to 90 % at 300 ppm. The PP data showed that this drug acts as mixed mode mechanism. From the EIS examination, we notice the decrease in the values of double layer by increasing the dose of Erdosteine drug, on the other hand, the charge transfer resistance is increased. Thermodynamic parameters of activation and adsorption processes were calculated and discussed. The sign of the free energy of adsorption showed spontaneous process of adsorption and the stability of the adsorbed film. The surface morphology of the SS304L samples was estimated utilizing “Atomic Force Microscopy (AFM), X-ray photoelectron spectroscopy and Fourier transform infrared spectroscopy (FTIR)”. Results gain for all tests used are in good agreement. To study the stability of Erdosteine and its interaction with solvent at different time intervals, different solvation thermodynamic parameters were determined from; density, refractive index and UV-spectra measurements.

Keywords: SS304L, Corrosion inhibition, HCl, AFM, FTIR, Erdosteine drug, Solvation

Introduction

Corrosion is a chemical or electrochemical attack that causes deterioration of engineered materials' physical, metallurgical, and mechanical properties. It's one of the 'hereditary diseases' of metals and their alloys, and it can be localized or uniform. SS 304L is the basic chromium-nickel stainless steel which has determined extensive programs in kind of industries due to its critical traits including versatility, durability and excessive mechanical and corrosion resistance [1]. The failure of SS resulting from pitting corrosion is a serious technological problem. Pitting corrosion occurs as a result of the breakdown of the oxide film in an aggressive acidic medium [2]. It is notable that

corrosion never stops however its extension and seriousness can be brought down. However, corrosion control is a fundamental issue from an application standpoint, and it has been determined that inhibitors should have been used, which act as a barrier to reduce the environment's aggressiveness against corrosion [3–7]. Among the acid solutions, hydrochloric acid is one of the most widely used regular aggressive solutions [8–9]. To control the attack of acid on the base metal surface, the use of efficient inhibitors in hydrochloric acid is essential. The inhibitors used in such cases should be effective even under severe conditions in concentrated hydrochloric acid and temperatures ranging from 273 to 333 K [10].

*Corresponding author e-mail: feldossoki64@gmail.com (Farid El-Dossoki)

Receive Date: 05 April 2022, Revise Date: 28 April 2022, Accept Date: 09 May 2022

DOI: 10.21608/EJCHEM.2022.131748.5806

©2022 National Information and Documentation Center (NIDOC)

Heterocyclic compounds such as antibiotic (pharmaceutical drugs) can provide excellent inhibition. These molecules depends at most on certain physical properties of the inhibitor molecules such as functional groups, steric factors, electron density at the donor atom and electronic structure of the molecules [11]. A few researchers have been remind the use of antibacterial drugs as corrosion inhibitors because of presence of oxygen, nitrogen and sulphur in their structures as active centres, high solubility in water, high molecular size, non-toxic and environmentally friendly corrosion inhibitors, important in biological reactions, also drugs can be easily produced and purified as a corrosion inhibitor for high carbon steel in hydrochloric acid solution such as: pantoprazole sodium [12], sulfa drug [13], clindamycin antibiotic [14], pyridine and its derivatives [15], Rhodanine [16], levofloxacin [17], cephalosporin [18], methionine [19]. In present years the use of drugs as corrosion inhibitors for different metals namely Cefatrexyl, Ciprofloxacin, Norfloxacin, Ofloxacin drugs, Tacrine have paid attention on by some authors [20–22].

Erdosteine is an antibiotic useful for help clear sputum in adults with chronic bronchitis [31]. The goal of this study is to analyse the corrosion behaviour of SS304L in 1M HCl at altered temperatures and doses by altered tests (chemical and electrochemical tests). The surface morphology of the SS304L specimens also analysed and discussed.

2. Experimental techniques

2.1. Materials

The chemical composition of 304L SS (in weight %) seen in (Table 1). “For chemical measurements, 304L SS specimen with an exposed surface area of 2 x 2 x 0.2 cm was used and for electrochemical tests, the exposed surface area of metal was 1 cm². Prior to each experiment, the surface of 304LSS specimens was abraded with the finest grade emery papers to mirror finish, rinsed with acetone and finally washed with doubly distilled water”.

Inhibitor (drug)	Sample	Medium	IE %	References
Pencillin G (15x10⁻⁴M)	Mild steel	H ₂ SO ₄	90.0	[23]
Penicillin V (15x10⁻⁴M)	Mild steel	H ₂ SO ₄	63.3	[24]
Cefalexin (11x10⁻⁴M)	Mild steel	HCl	67.5	[25]
Ceftriaxone (400 ppm)	Mild steel	HCl	87.6	[26]
Ketamine (300 ppm)	316 SS	HCl	94.0	[27]
Augmentine (300 ppm)	Carbon steel	HCl	97.8	[28]
Desloratadine drug (2000 ppm)	steel	HCl	92.2	[29]
amoxicillin (500 ppm)	Sabic iron	HCl	88.4	[30]

Table 1. Chemical conformation (weight %) of the 304L SS

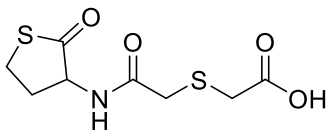
Element	C	Si	Mn	Cr	P	N	Ni	Fe
Weight (%)	0.03	0.75	2.0	18-20	0.045	0.1	8.00/12.0	the rest

2.2. Inhibitor and chemicals

The pharmaceutical compound has been examined named Erdosteine which purchased from Eipico company, Cairo, Egypt. The investigated pharmaceutical drug is used as received and chosen because: it is easily soluble in water, has high molecular weight, save corrosion inhibitor, contains donating atoms (N, O and S), and, important in biological reactions and easily available. All the solutions were prepared from AR

grade chemicals using bi-distilled water. The aggressive solutions used were made from 37 % HCl, appropriate doses of acid were prepared using bi-distilled water. 1000 ppm stock solutions from the investigated drug were prepared by dissolving one gram /liter of the solid pharmaceutical drug in bi-distilled water; the other doses of pharmaceutical drug (50 – 300 ppm) were prepared by dilution with bi-distilled water”. All the materials utilized were of AR grade and utilized as received.

Table 2 Molecular structure, formula and weight of investigated drug

Inhibitor	Structure	Mol. Formula	Mol. Weight
Erdosteine		C ₈ H ₁₁ NO ₄ S ₂	249.30

2.3. Methods

2.3.1. Chemical measurements

A. Weight Loss (WL) Measurements

Coupons of SS304L specimens of size $2 \times 2 \times 0.2$ cm were weighed and immersed in 100 ml of the test solution in open beakers. "The beakers were placed into a water bath maintained at 25°C. Each sample of SS304L was withdrawn from the test solution after every 30 min, washed and dried in air before reweighing. The difference in weight after each interval was taken as the WL. The experiment was repeated utilized by ASTM practice standard G-31 Standard practice for laboratory immersion corrosion testing of metals, ASTM International, 2004). From the WL results, the inhibition efficacy (% IE) of the drug, degree of surface coverage (θ) and corrosion rate (k_{corr}) were determined using the following equations" [32,33]:

$$\% \text{ IE} = \theta \times 100 = [1 - (W_1/W_2)] \times 100 \quad (1)$$

$$k_{\text{corr}} = W / At \quad (2)$$

where " W_1 and W_2 are the WLs for SS304L in the presence and absence of the drug, A is the area of the SS304L coupon (cm^2), t is the time of immersion (min) and W is the WL (mg cm^{-2})" of SS304L after time t (min).

2.3.2. Electrochemical measurements

A three electrode electrochemical cell was used. "The working electrode was SS304L of surface area of 1 cm^2 . Before each experiment, the electrode was abraded using emery papers as before. After this, the electrode was cleaned ultrasonically with ethyl alcohol and washed by bi-distilled water. All potentials were given with reference to the saturated calomel electrode (SCE). The counter electrode was a platinum plate of surface area of 1 cm^2 . The working electrode was immersed in the test solution for 30 min until a steady state open circuit potential (E_{ocp}) was obtained. The polarization curves were recorded by polarization from -0.6 V to 0.2 V under potentiodynamic conditions corresponding to 1 mV/s (sweep rate) and under air atmosphere [34-36]. All measurements were carried out with SS304L electrode in 1M HCl in the absence and presence of different doses of the investigated drug at 25°C. All experiments were carried out at 25°C. The %IE and (θ) were calculated from the following equation:

$$\% \text{ IE} = \theta \times 100 = [1 - (i_{\text{corr(inh)}} / i_{\text{corr(free)}})] \times 100 \quad (3)$$

Where " $i_{\text{corr(free)}}$ and $i_{\text{corr(inh)}}$ are the corrosion current densities in the absence and presence of inhibitor", respectively.

"Electrochemical impedance spectroscopy measurements were performed using the same cell that used in PP experiments. The EIS carried out over a frequency range of 1 Hz to 100 kHz, with a signal amplitude perturbation of 10 mV. The (% IE) and (θ) of the investigated drug obtained was calculated from the following equation":

$$\% \text{ IE} = \theta \times 100 = [1 - (R_{\text{ct}}^{\circ} / R_{\text{ct}})] \times 100 \quad (4)$$

Where R_{ct}° and R_{ct} are the charge transfer resistance values in the absence and attendance of the inhibitor, correspondingly.

All electrochemical measurements were carried out using "Potentiostat /Galvanostat / Zra analyser (Gamry PCI4-G750). A personal computer with DC105 software for PP, and EIS300 software for EIS and Echem Analyst v 5.21" was used for data fitting.

2.3.3. Surface Examinations

The specimens of SS304L used for surface morphology examination were immersed in "1M HCl in the absence (blank) and presence of 300 ppm of Erdosteine at 25°C for 1day. The analysis was performed using atomic force microscopy (AFM) by used on a Pico SPM2100 AFM device operating in contact mode in air at Nanotechnology Laboratory, Faculty of Engineering Mansoura University. IR Affinity (Perkin-Elmer) spectrophotometer was used for recording the FTIR spectra to determine the composition of the corrosion product formed on the SS304L surface. It can perform the surface characterization XPS by utilizing monochromatic X-ray Al K-alpha radiation of (10-1350 eV) and spot size of 400 with full spectrum pass energy of (200 - 50eV)".

2.5. Biological Effect

Erdosteine was utilized for testing its ability to prohibit the growth of bacteria in cooling tower of ammonia at Talkha factory for fertilizers by implementing the spore suspension procedure. "By separating this bacteria and cultivate it in a plate over nutrient agar then after growth, taking numerous swaps from several collected colonies then multiply it in 1L measuring flask containing deionized water. Then left it for 1-3/2 hrs before cultivating again (with adding Erdosteine). Then left it for 1/2 - 1 hr then

taking 2 ml from this solution by syringe and pouring over agar solution in two cultivating plates; one without Erdosteine, the other containing the 300 ppm and waiting for maximum 2 days. The plates were incubate at 310K then counting colonies by UVP colony DOC". It apparatus, the plates exhibited suitable resistance to the bacteria.

2.6. Quantum chemical calculations

To observe the correlation among the molecular structure and the reactivity of Erdosteine compound, theoretical calculations had been performed the use of DMol3 module installed in Materials Studio model 7.0.

2.7. Monte Carlo (MC) simulations

MC simulations were achieved using Materials Studio 7.0 (Accelrys Inc., San Diego, CA, USA) in a simulation box with periodic boundary conditions. A pure iron crystal was introduced and cleaved along the most stable (less energy) plane (1 1 0) constructing a 30 Å vacuum slab. The plane surface of Fe (1 1 0) has been relaxed by decreasing its energy; this step has been followed by extending the surface of Fe (1 1 0) to a super cell (10 / 10). The simulation analysis was performed in a test box containing the simulated corrosive species and one molecule of each inhibitor using the Monte Carlo quest and assigning the COMPASS force field known as a high-quality force field to combine parameters of inorganic and organic materials"

3. Results and Discussion

3.1. Chemical Measurements

3.1.1 WL Measurements

WL of SS304L was determined, at various time intervals, in the absence and attendance of altered doses of Erdosteine. "From the experimental data of the WL measurements, the % IE, was calculated from equation (1), All the experiments were performed at 25-45°C. Values of corrosion rates (k_{corr}) and % IE of Erdosteine are summarized in (Tables 3). The value of % IE increases with increasing drug doses and decreases with rise in temperature. This behaviour can be attributed to the increase of the surface coverage and due to the adsorption of drug on the surface of SS304L. The optimum dose wanted to achieve an efficiency of 90% was found to be 300 ppm. In all cases, the increase in the inhibitor dose was accompanied by a decrease in WL and an increase in the percentage inhibition. These results lead to the conclusion that the Erdosteine under investigation are fairly efficient as inhibitor for SS304L dissolution in HCl solution. The results confirmed the very good effect of Erdosteine drug on the corrosion inhibition of SS304L in 1M HCl solution as corrosive media. Fig. 1 shows the WL-

time curves for the corrosion of SS304L in 1M HCl solution in the absence and presence of Erdosteine drug at 25°C".

3.1.2 Effect of Temperature

The effect of temperature on the corrosion parameters of SS304L with the addition of Erdosteine drug was studied using WL method. "A major advantage of this method is its relative simplicity and availability. The data of corrosion behaviour of SS304L in 1M HCl containing different doses of Erdosteine for 120 min in temperature range 25-45°C were presented in (Table 3). Inspection of this Table revealed that the k_{corr} of SS304L increases with increasing temperature. On the other hand, the %IE of Erdosteine decreased with raising temperature Fig. 2. This suggested possible desorption of some of the adsorbed drug molecules from the metal surface at higher temperatures. Such behaviour shows that the drug was physically adsorbed on the metal surface".

Arrhenius-type dependence is detected among k_{corr} and temperature often stated as:

$$k_{\text{corr}} = A \exp -E_a^*/RT \quad (5)$$

Where " E_a^* is the apparent activation energy, R is the universal gas constant, T is the absolute temperature, and A is the frequency factor. Fig. 3 depicts Arrhenius plot $\log k_{\text{corr}}$ against the reciprocal of temperature 1/T for SS304L in 1M HCl solution in the absence and presence of different Erdosteine doses". An alternative formulation of Arrhenius balance Eq. is [37]:

$$k_{\text{corr}} = RT/Nh \exp (\Delta S^*/R) \exp (-\Delta H^*/RT) \quad (6)$$

Where "h is the Planck's constant and N is the Avogadro's number.

Fig. 4 shows a plot of $\log k_{\text{corr}}/T$ as a function of 1/T for SS304L. Straight lines were obtained with a slope of $-\Delta H^*/R$ and an intercept of $\ln R/Nh + \Delta S^*/R$ from which the values of ΔH^* and ΔS^* were calculated for the blank and Erdosteine. The values of the E_a^* , ΔH^* and ΔS^* were recorded in (Table 4).

The increase in the E_a^* is proportional to the drug dose, indicating that the energy barrier for corrosion process is also increased [38].

The increase in the ΔH^* in presence of the drug means that the addition of the Erdosteine to the acid solution increases the height of the energy barrier of the corrosion reaction to an extent depends on the type and dose of the present Erdosteine.

The adsorption of the drug molecules on the metal surface leads to a lower number of hydrogen atoms adsorbed on it; this will cause a decrease in hydrogen

evolution rate rather than the rate of metal dissolution, because of the blocking of the surface of the metal by the drug molecules”.

Table 3 Corrosion rate (k_{corr}) and %IE data gotten from WL tests for SS304L in 1M HCl solution in the absence and attendance of altered doses of Erdosteine at 25°C

Conc., ppm	(k_{corr}), $\text{mg cm}^{-1}\text{Min}^{-1}$	θ	% IE
Blank	0.051	----	----
50	0.010	0.804	80.4
100	0.009	0.824	82.4
150	0.0081	0.841	84.1
200	0.007	0.863	86.3
250	0.0062	0.878	87.8
300	0.0047	0.908	90.8

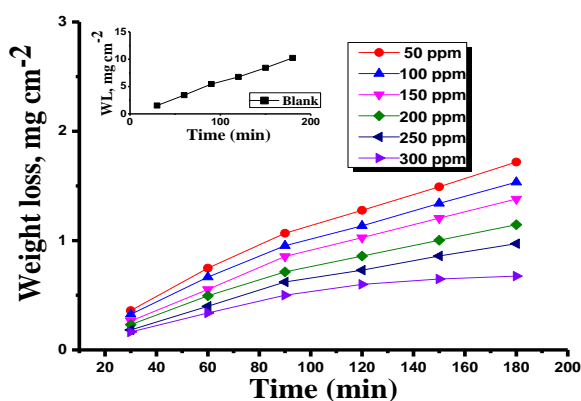


Fig. 1. Time-WL curves for the SS304L dissolution in 1M HCl solution in the absence and attendance of altered doses of Erdosteine drug at 25°C

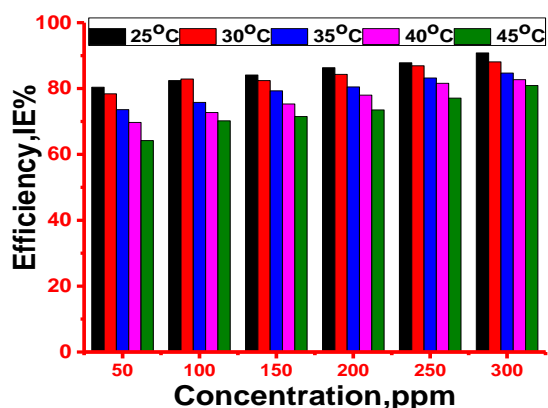


Fig. 2. Effect of doses on the %IE of Erdosteine at altered doses.

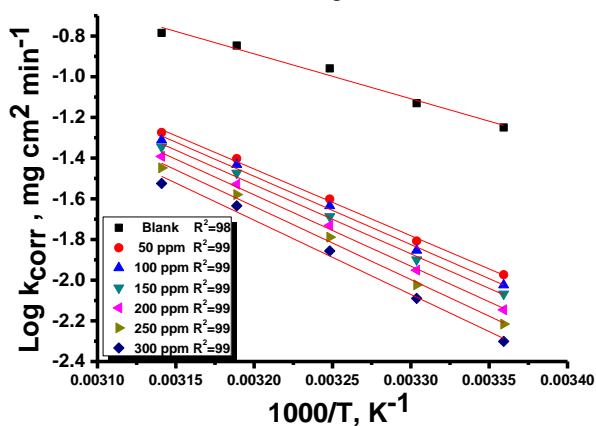


Fig. 3. Arrhenius plots for the k_{corr} of SS304L in 1M HCl with and without Erdosteine at altered temperatures

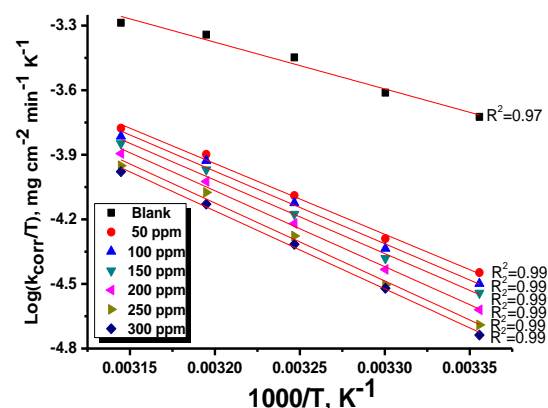


Fig. 4. $\text{Log}(k_{\text{corr}}/T)$ versus $1/T$ for SS304L in 1M HCl as blank and with Erdosteine at altered temperatures

3.1.3 Adsorption Isotherms

Erdosteine drug adsorbed on the SS304L surface and the data of (θ) for change doses of drug in 1 M hydrochloric acid were determined from WL data utilizing the follows Eq. (1). “ θ values were increased

with raising the Erdosteine doses. By utilizing these data and for applying altered adsorption isotherms, Langmuir adsorption isotherm was recognized to be the best explanation of the inhibitor adsorption behaviour on the surface of SS304L and the regression

constant ($R^2=0.99$) reach to unity and to obey the next Eq.” [39].

$$C/\theta = 1/K_{ads} + C \quad (7)$$

Where, “C, K_{ads} express on the dose and equilibrium constant of adsorption procedure, respectively. Drawing (C) vs. (C/θ) of Erdosteine drug at change temperatures was presented in Fig. 5. The intercept equal to (1/ K_{ads}) and slope similar the unity”, the adsorption constant give result to the ΔG^0_{ads} by next:

$$K_{ads} = (1/55.5) \exp (\Delta G^0_{ads} / RT) \quad (8)$$

The ΔG^0_{ads} data at all temperatures are documented in Table 5. The (ΔH^0_{ads}) was measure agreeing to the Van't Hoff eqn.

$$\log k_{ads} = \left(\frac{-\Delta H^0_{ads}}{2.303RT} \right) + constant \quad (9)$$

Plotting “(log K_{ads}) vs. (1/T) give straight line as displayed in Fig. 6, the slope = ($-\Delta H^0_{ads}/2.303R$), from this slope; the ΔH^0_{ads} data was calculated and is recorded in Table 5”. Then by applying the next balance:

$$\Delta G^0_{ads} = \Delta H^0_{ads} - T\Delta S^0_{ads} \quad (10)$$

Table (5) shows the adsorption parameters for the obtained Erdosteine drug. “The data of the table

Table 4. Activation parameters of SS304L corrosion in the absence and attendance of various doses of Erdosteine in 1M HCl

Conc.,ppm	Activation parameters		
	E_a^* kJ mol ⁻¹	ΔH^* kJ mol ⁻¹	$-\Delta S^*$ J mol ⁻¹ K ⁻¹
Blank	41.1	38.5	130.2
50	61.3	58.8	72.9
100	62.9	60.1	68.5
150	63.8	61.1	66.5
200	65.8	63.5	60.5
250	67.4	64.8	55.8
300	68.5	65.9	53.9

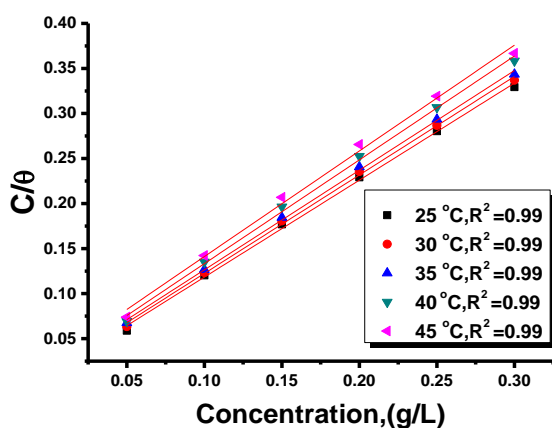


Fig. 5. Langmuir isotherm for Erdosteine adsorption on SS304L surface in solution from 1 M hydrochloric acid at altered temperatures

confirmed the spontaneous adsorption of Erdosteine drug on the SS304L surface, through the negative data obtained ΔG^0_{ads} , whose negative value lowered with higher temperature, which confirms that the adsorbed layer is more stable at lower temperatures. The results gotten from free energy confirm that the type of adsorption incident is physical adsorption and not chemical as it is known that ΔG^0_{ads} values when they are less than -20 kJ / mol are physical adsorption. Where these results established that the adsorption is physisorption. The value of enthalpy is negative, which means that adsorption molecules of drug are exothermic. The exothermic process can refer to physical or chemical adsorption, but the value governs the kind of adsorption. ΔH^0_{ads} value less than 40 kJ/mol refer to the physisorption process”. The ΔS^0_{ads} values are positive due to the rise of disorder because desorption of water molecules from the surface of SS 304[40].

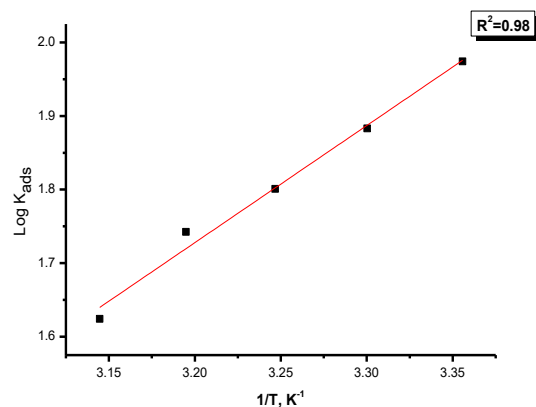


Fig. 6. (Log K_{ads}) vs. (1/T) for the dissolution of SS304L in 1M HCl in the existence of Erdosteine drug at altered temperatures

Table 5. Parameters of Langmuir adsorption of Erdosteine on the SS304L surface at change temperatures

Temp °C	$-\Delta G^{\circ}_{\text{ads}}$, kJ mol ⁻¹	$-\Delta H^{\circ}_{\text{ads}}$ kJ mol ⁻¹	$\Delta S^{\circ}_{\text{ads}}$ J mol ⁻¹ K ⁻¹
25	19.2	27.0	73.1
30	19.0		71.3
35	18.9		69.7
40	18.8		68.6
45	18.5		66.4

3.2. Electrochemical measurements

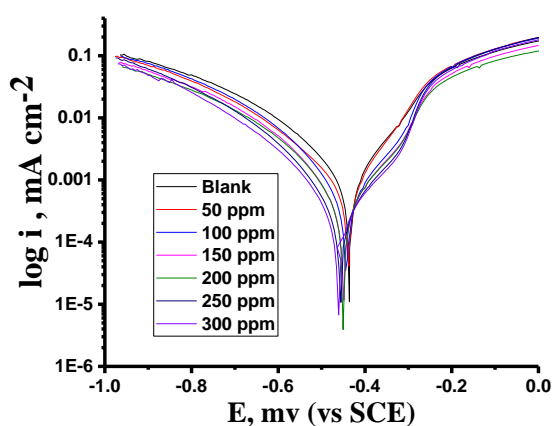
3.2.1 PP Measurements

The cathodic and anodic polarization curves for SS304L in 1 M HCl solution in uninhibited and inhibited solutions of Erdosteine at 25°C are shown in Fig.7. “The various electrochemical parameters calculated from Tafel plots are given in Table 6. It is clear that the investigated inhibitor promotes the retardation of anodic dissolution of SS304L and cathodic hydrogen discharge reactions. It is observed that the presence of Erdosteine on the SS304L, while the E_{corr} and Tafel slopes experience no significant

change in the inhibited solution compared to the uninhibited solution. The addition of Erdosteine caused no considerable shift in the E_{corr} values, suggesting that the drug acts as a mixed-mode inhibitor [41-43]. The results show also that the slope of the anodic and the cathodic Tafel slope was slightly changed on increasing the dose of the investigated drug. This indicates that there is no change in the mechanism of inhibition in presence and absence of drug. The higher values of Tafel slope can be attributed to surface kinetic process rather the diffusion-controlled process” [44]

Table 6. Effect of Erdosteine doses on corrosion parameters of 304L SS in 1M HCl at 25°C

Conc, ppm	i_{corr} , $\mu\text{A cm}^{-2}$	$-E_{\text{corr}}$, mV vs SCE	β_a , mV dec ⁻¹	β_c , mV dec ⁻¹	k_{corr} , mpy	θ	% IE
0.0	1420	436	139	185	558	--	--
50	620	439	128	191	428	0.563	56.3
100	432	443	140	188	266	0.696	69.6
150	284	449	135	188	207	0.800	80.0
200	250	450	140	187	185	0.824	82.4
250	205	457	141	181	138	0.856	85.6
300	154	461	138	183	111	0.892	89.2

**Fig.7.**Tafel polarization curves of 304L SS dissolution with and without altered doses of Erdosteine at 25°C

3.2.2 EIS Measurements

Figure 8 shows the Nyquist plot for SS304L in 1M HCl in the absence and attendance of different doses of Erdosteine at 25°C. “This diagram has a semicircle appearance; it indicates that the corrosion of

Erdosteine is mainly controlled by a charge transfer process. The Bode plot for the SS304L is shown in Fig. 9 where the high frequency limit corresponds to electrolyte resistance R_{Ω} , while the low frequency limit represents the sum of $(R_{\Omega} + R_p)$ where R_p is the first approximation determined by both the electrolytic conductance of the oxide film and polarization resistance of the dissolution and passivation process. Various impedance parameter such as charge transfer resistance (R_{ct}), double layer capacitance (C_{dl}) and (% IE) were calculated and are given in (Table 7). The data obtained showed that the values of charge transfer resistance (R_{ct}) increase and the values of layer (C_{dl}) capacitance double decrease with increasing the dose of the drug which accompanied with increasing (% IE), due to the adsorption of this drug molecules on the electrode surface leading to a film formation on Erdosteine surface. The obtained Nyquist impedance diagram in most cases does not show perfect semicircle. This may be attributed to the frequency dispersion as a result of the heterogeneity of the electrode surface” [45-47].

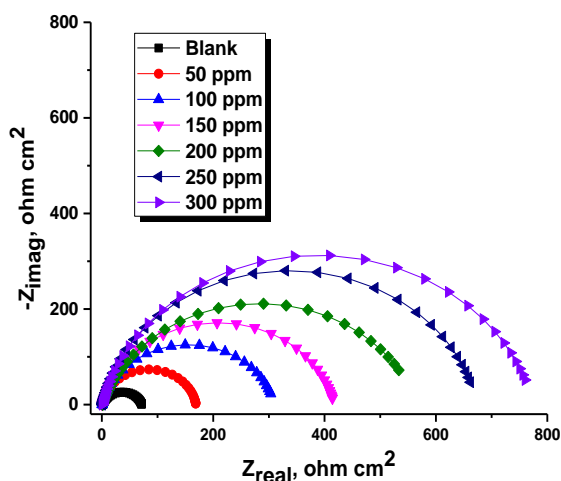


Fig. 8. Nyquist curves for the dissolution of SS304L

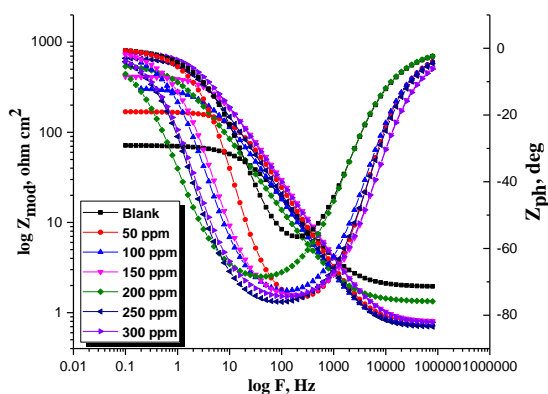


Fig. 9. Bode curves for the dissolution of SS304L in 1M HCl in the absence and presence of altered doses of Erdosteine at 25°C and Equivalent circuit model utilized to fit the impedance spectra.

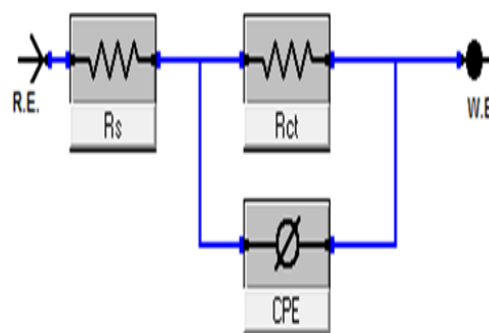


Table 7. EIS data for dissolution SS304L in 1M HCl in the absence and presence of altered doses of Erdosteine at 25°C

Conc, ppm	$Y_0, \mu\Omega^{-1} s^n cm^{-2} \times 10^{-6}$	n	$R_p, \Omega cm^2$	$C_{dl}, \times 10^6 \mu F cm^{-2}$	θ	% IE
0.0	255	0.867	69	137	----	----
50	138	0.912	168	97	0.589	58.9
100	122	0.866	294	73	0.765	76.5
150	118	0.836	416	66	0.834	83.4
200	111	0.818	564	60	0.878	87.8
250	103	0.824	673	58	0.897	89.7
300	88	0.838	740	52	0.907	90.7

3.3 Surface Examinations:

3.3.1 AFM analysis

AFM tests supplies photos with atomic or near-atomic-resolution surface topography which able to giving the surface roughness of coupons by the angstrom-scale. "Atomic force microscopy (AFM) is a very higher resolution type of scanning probe microscopy on the order of fractions of a nanometer,

in 1M HCl in the absence and presence of altered doses of Erdosteine at 25°C

more than 1000 times better than the optical diffraction limit [48]. Fig.10a shows the three dimensional (3D) AFM morphologies for polished SS304L surface as standard sample, Fig.10b SS304L surface immersed in 1M HCl as blank sample and Fig.10c SS304L surface immersed in 1M HCl +300 ppm of Erdosteine drug. The values Average roughness (S_a) nm show that the surface of the metal

is smoothed by the adsorbed surface layers of Erdosteine drug on the SS304L surface. It is clear that the lower roughness was detected on the free sample. The height and the roughness of the metal with Erdosteine is less compared with the height and the roughness of the blank sample". As the roughness decrease this indicate that the inhibitor made highly percent of inhibition against corrosion.

3.3.2 FTIR analysis

FTIR spectroscopy presentations exciting capabilities such as excessive signal to noise ratio, excessive sensitivity and selectivity, accuracy, "mechanical simplicity, short analysis time and small amount of sample required for the analysis. Fig.11 shows the FTIR spectra of the Erdosteine inhibitor. The finger print spectra of the stock drug and the SS304L surface after immersion in 1M HCl + 300 ppm of Erdosteine for 6 hours was obtained and compared to each other it was obviously clear that the same finger print of drug stock solutions present on SS304L surface except the absence of some functional group and it suggested to be due to reaction with HCl. From Fig.11 there are small shift in the

peaks at SS304L surface from the original peak of the stock drug solution, these shifts indicate that there is interaction between SS304L and inhibitor molecule".

3.3.3. XPS analysis

X-ray photoelectron spectroscopy (XPS) examination was achieved to check the Erdosteine adsorbed studied on the surface of 304L SS and define the chemical nature of Erdosteine / SS304L interface and the results were discussed as below. "The high-resolution XPS survey gotten from 304L SS surface dissolution in 1.0 M hydrochloric in the attendance of Erdosteine is demonstrated in Fig. 12. All spectra found from XPS display the forms of complex, which were dispersed to the binding energies (BE, eV) and the conforming quantification (%) of each peak constituent are recorded in Table 8. The XPS gotten from dissolution of SS304L in the attendance of the drug inhibitor studied, the XPS contains elements (Fe 2p, Cr2p, O 1s, Cl 2p, C 1s) in addition to N 1s core level as shown in Fig.12 [49]. All that approve the Erdosteine inhibitor adsorbed on the SS304L in acidic environment".

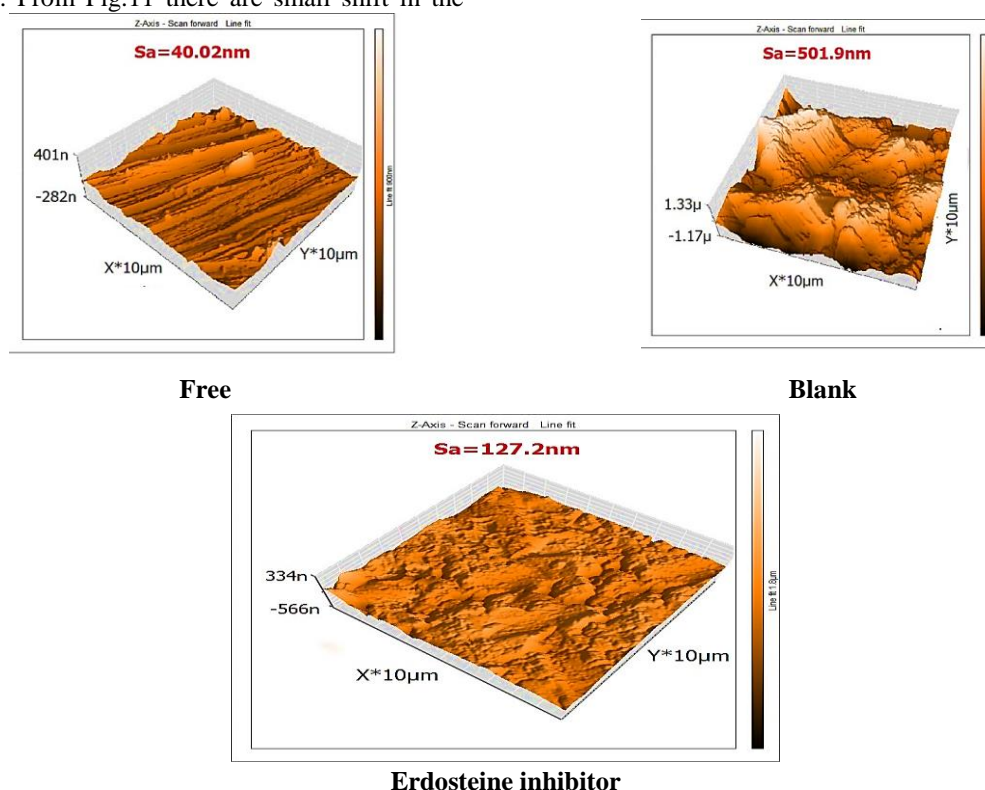


Fig. 10. AFM analysis on SS304L in attendance and absence of Erdosteine drug for 1 day's immersion

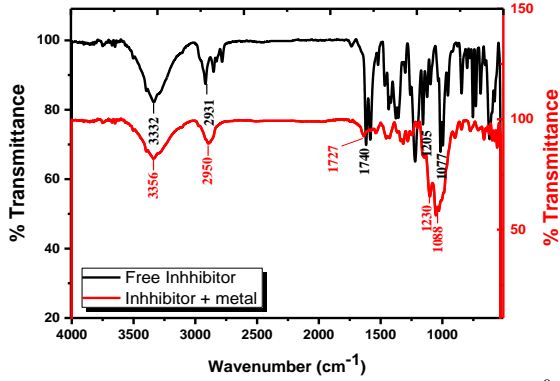
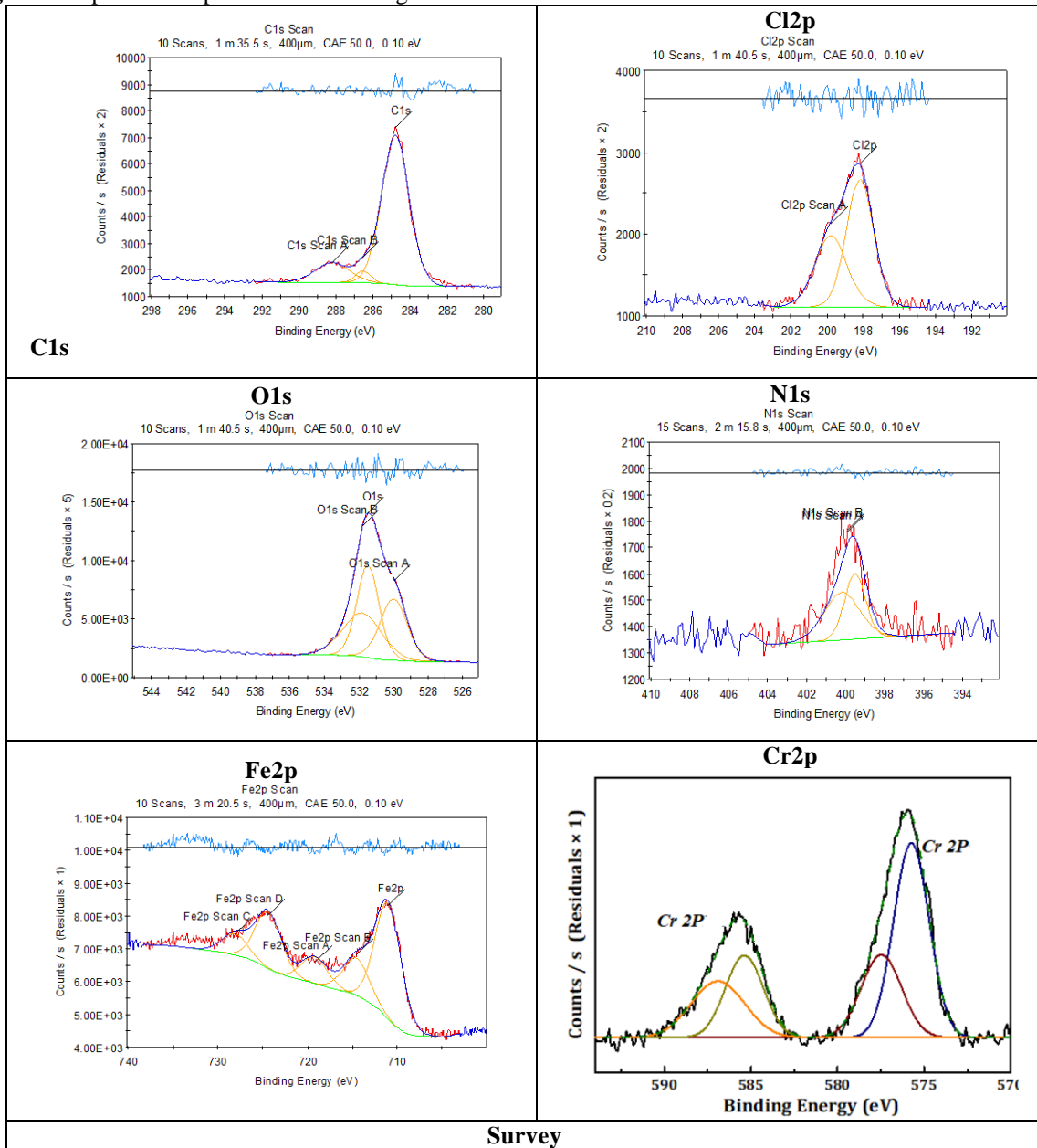


Fig. 11. IR spectrum of pure Erdosteine drug at 25 °C



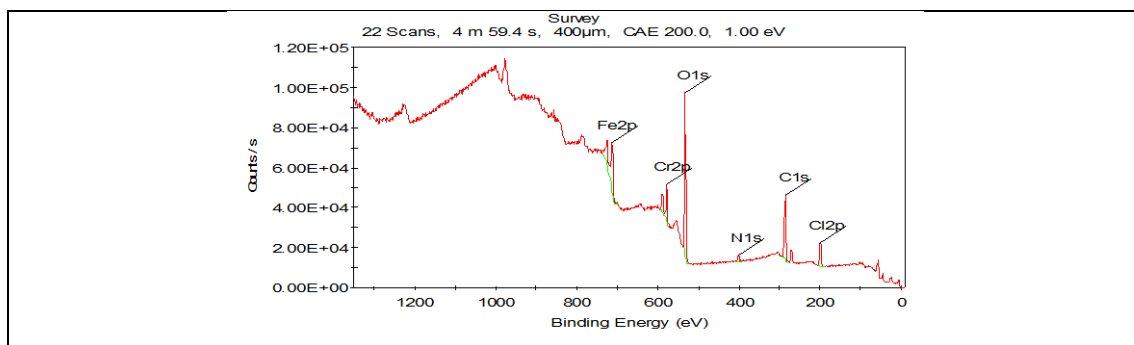


Fig. 12. XPS graphs of (a) XPS survey, (b) C1s scan, (c) Cl2p scan (d) O1s scan(e) N1s scan(f) Fe2p scan(g) Cr2p scan of SS304L after immersion in 1 M HCl+300ppm of Erdosteine inhibitor for 24 h.

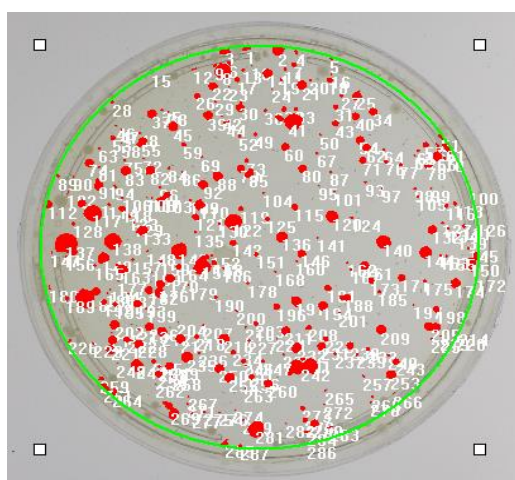
Table 8. Binding energies of surveys and its expected bonds.

Core element	BE, eV	Assignments
C1s	286.87	C-H, C-C, C-O, C+-O, C=O
	287.20	
	285.54	
Cl2p	198.18	Cl 2p _{3/2}
O1s	536.42	Fe ₂ O ₃ , Fe(OH) ₂
N1s	405.87	Cu-Nx.
Fe2p	711.03	Fe ₂ O ₃ , FeOOH, FeCl ₃
	716.22	
	728.09	
Cr2p	585.81	Cr ₂ O ₃ , Cr(OH) ₃
	574.12	

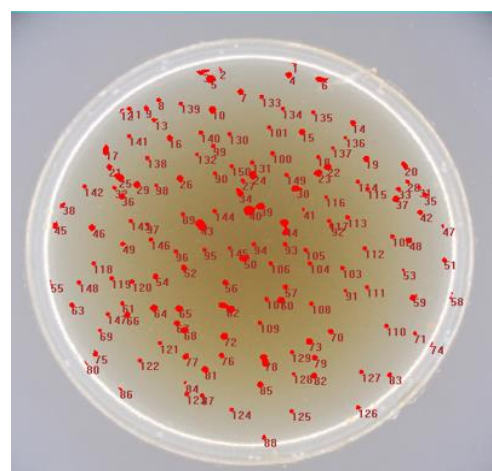
3.4. Biological effect

Biological effect of acute toxicity tests was done for Erdosteine drug using Doc-it colony instrument. “The photos of bacteria colonies using the instrument, for blank and for Erdosteine were demonstrated in Fig.13. The number of bacteria colonies cultivated obtained

using Doc-it colony instrument was shown in Table 9. The results of Table 9 show that the number of bacteria colonies for Erdosteine (150 colonies) was lesser than the blank (297 colonies), meaning that Erdosteine has a kindly impact in preventing multiplying bacteria, and so the CR decreased”.



(a) photo by Doc-it instrument for blank



(b) photo by Doc-it instrument for AE

Fig. 13. Original photos of bacteria colonies by Doc-it colony for (a) blank and (b) Erdosteine.

Table 9. Number of bacteria colonies for blank and for Erdosteine as obtained using Doc-it colony counter instrument

Sample	No of bacteria colonies
Blank	297
Erdosteine	150

3.5 Quantum Chemical Parameters

The quantum chemistry, “according to the DMol3 module established in Materials Studio version 7.0 software was utilized for all calculations in the current research. The analysis of the density distributions optimized geometry, highest occupied molecular orbital (HOMO), and lowest unoccupied molecular

orbital (LUMO) structures of the inhibitors are shown in Figure 14. HOMO and LUMO can determine the donation - acceptance capacity and the molecular reactivity of the Erdosteine drug. E_{HOMO} denotes the ability of the molecule to donate electron, whereas E_{LUMO} describes the ability of the molecule to accept electron. The dipolar moment (μ) is a measure of the polarity with the covalent bond. The energy band gap ΔE_g ($\Delta E = E_{HOMO} - E_{LUMO}$) that the lower energy gap value is considered to be high reactivity molecule and have a good corrosion inhibition efficiency onto the metal surface [50]. The (μ) calculated the polarity with the covalent bond between the compounds studied. It is accepted that the high μ values improve the adsorption tendency on metal surface of the compounds tested”.

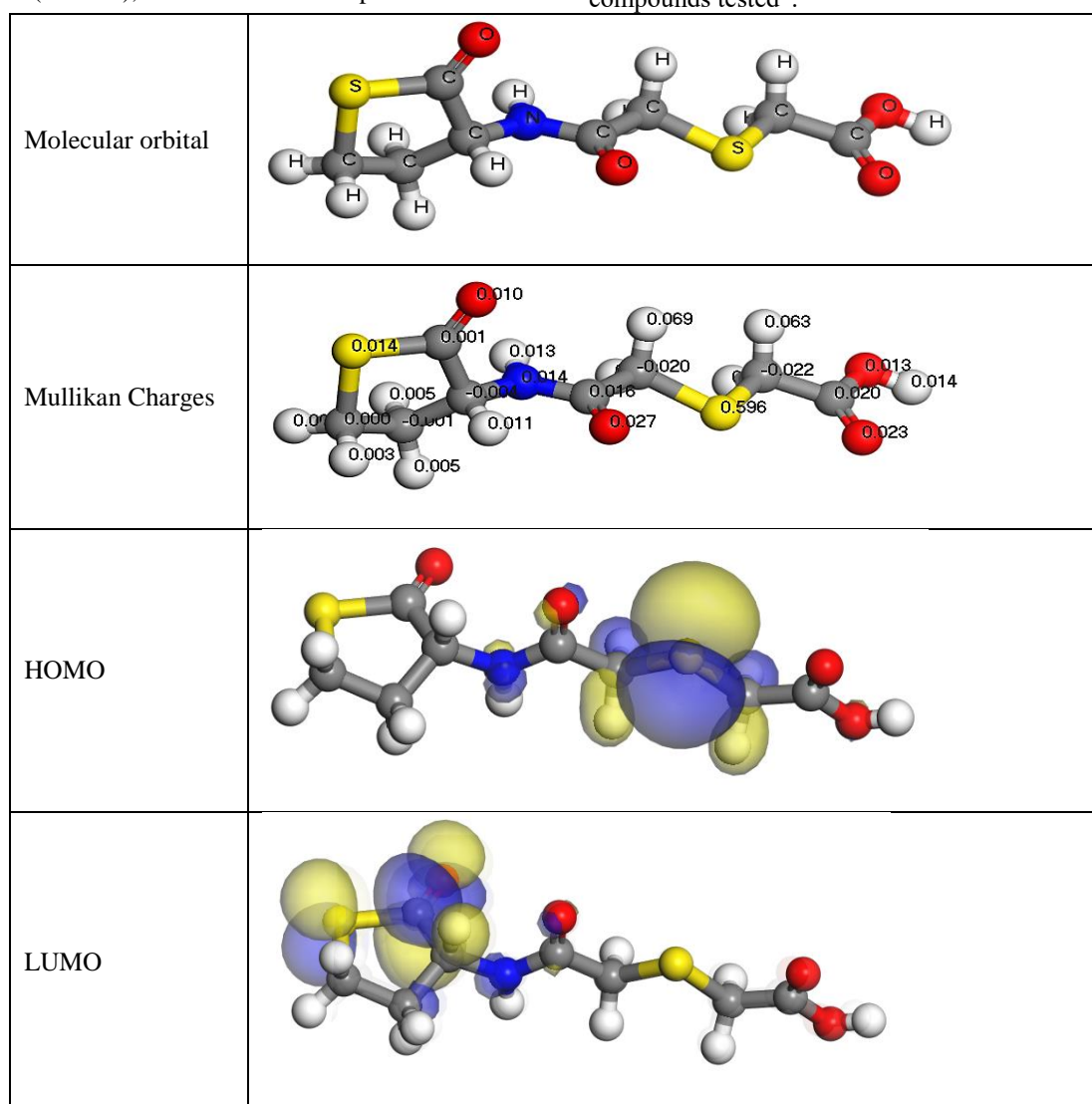


Fig. 14. The frontier molecular orbital Erdosteine inhibitor (HOMO and LUMO).

Table 10. Parameter gotten from quantum for Erdosteine drug

Parameters (Variable)	DMol3
E_{HOMO} (eV)	-5.29
E_{LUMO} (eV)	-1.64
ΔE , (eV) ($E_{\text{L}}-E_{\text{H}}$)	3.65
μ (debye) (Dipole moment)	10.07

3.9. Monte Carlo (MC) Simulation

The side and top observations of the most suitable adsorption formations for the “Erdosteine drug tested on the SS304L surface obtained from the adsorption locator module are thus shown in Table 11. Adsorption energy is characterized as declining energy, when two materials are mixed during the adsorption process in Table 11. Results and descriptors measured by the Monte Carlo simulation for adsorption of Erdosteine molecule on iron (1 1 0).

which an electron, ion or molecule (adsorbent) is bound to the solid surface. As seen in Table 11, Erdosteine has higher energy for adsorption, which predicts the heavy adsorption of Erdosteine on the hardened surface of SS304L creating adsorbed stable layers which protecting the SS304L from corrosion”.

Structures	Total energy	Adsorption energy	Rigid adsorption energy	Deformation energy	Compound dEad/dNi	H ₂ O dEad/dNi
Fe (1 1 0)/ Erdosteine /H ₂ O	-1350.709	-1343.883	-1395.503	51.61	-106.55	-0.397

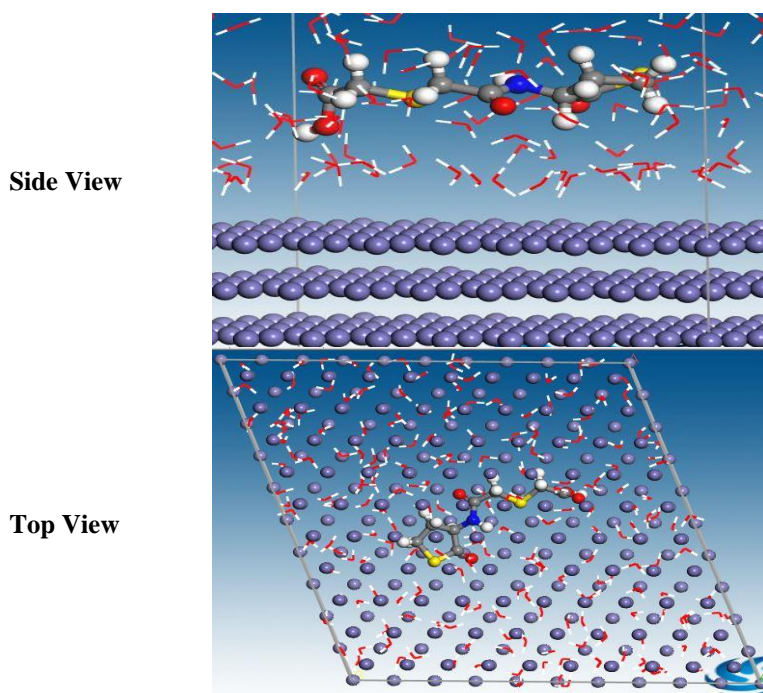


Fig. 15. The most appropriate conformation for adsorption of the Erdosteine molecule on Fe (1 1 0).

3.4. Mechanism of Corrosion Inhibition

The adsorption of drug molecules can be attributed to the existence of polar unit having atoms of nitrogen, sulphur, oxygen, and heterocyclic rings. “Therefore, the possible reaction centres are unshared electron pair of hetero-atoms and π -electrons of ring [51]. The adsorption and inhibition effect of drug molecules in 1M HCl solution can be explained as follows: In aqueous acidic solutions, drug molecules

exist either as neutral molecules or as protonated molecules and may adsorb on the metal/acid solution interface by one and/or more of the following ways: (i) electrostatic interaction of protonated molecules with already adsorbed chloride ions, (ii) interaction between unshared electron pairs of hetero-atoms and vacant d-orbital of iron surface atoms. The possible explanation of the inhibition is due to adsorption process which is considered as the key of the

mechanism of inhibition action. It might be proposed that the drug molecules adhere to the steel surface. The presence of a charged metal surface (304LSS in acid medium) is positively charged and species with charge in the bulk of the solution are required for the

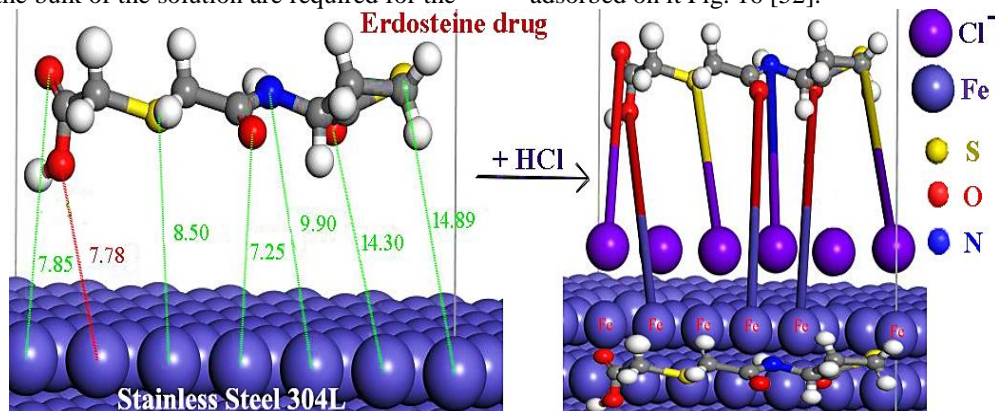


Fig. 16. Mechanism of inhibition

3.5. Solvation Properties of Erdosteine:

Solvation process describes the interaction of solvent with molecules or ions of a solute. Ions, and to some cases, molecules, interact strongly with solvent, and the strength and nature of this interaction influences many properties of the solute, including solubility, reactivity, molal volume and colour. In the process of solvation, ions are surrounded by concentric shells of solvent. Solvation is the process of reorganizing solvent and solute molecules into solvation complexes. Solvation involves bond formation, hydrogen bonding, and van der Waals forces. Solvation of a solute by water is called hydration. Solvation can be studied in terms of density, UV-spectra and refractive index measurements. Many interactions in solutions were considered depending on the solvation process of the substances as reported

earlier [53-54]. Also, density, refractive index and UV-spectra measurements of solutions are expected to shed some light on the solute-solvent interactions and configuration of their mixtures [55]. To study the stability of this compound and its interaction with solvent with time, different solvation thermodynamic parameters were done from; density, refractive index and UV-spectra measurements.

3.5.1-Effect of Solvent on the UV-Visible Spectra of Erdosteine:

The UV-Visible spectra of Erdosteine with concentration (1000 ppm) in ethanol-water mixed solvents at different time intervals were measured and represented in Figure (17, 18, and 19). The values of the absorbance and the wavelength of the Erdosteine are collected in Table 12.

Table 12: UV-visible spectra of Erdosteine (1000 ppm) in ethanol-water mixed solvents at different time intervals at 298 K°

EtOH% (Vol%)	0 hr.			24 hr.			72 hr.		
	peaks	λ (nm)	abs	peaks	λ (nm)	abs	peaks	λ (nm)	abs
Zero%	1	244	1.590	1	244	1.590	1	244	1.590
	2	279	1.191	2	279	1.191	2	279	1.191
30%	1	244	0.606	1	244	0.798	1	244	0.648
	2	281	0.104	2	282	0.206	2	281	0.204
50%	1	245	0.611	1	244	0.720	1	245	0.352
	2	282	0.1141	2	282	0.198	2	283	0.124
70%	1	243	0.0474	1	-	-	1	243	0.158
	2	286	0.036	2	198	-	2	286	0.043
90%	1	241	0.383	1	240	0.322	1	241	0.076
	2	320	0.035	2	313	0.033	2	320	0.025

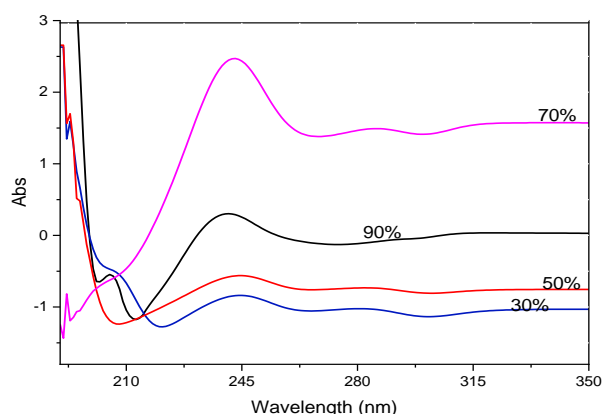


Fig. 17: UV-visible Spectra of Erdosteine in different mole fraction of ethanol-water mixed solvent (0, 30, 50, 70, 90%, Vol %) after time 0 hr.

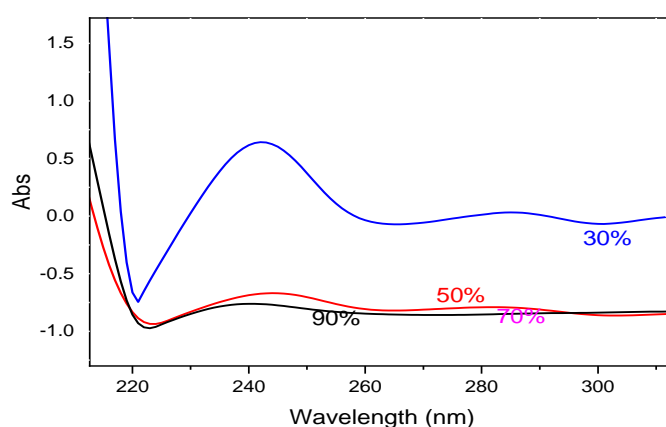


Fig. 18: UV-visible Spectra of Erdosteine in different mole fraction of ethanol-water mixed solvent (0, 30, 50, 70, 90%, Vol %) after time 24 hr.

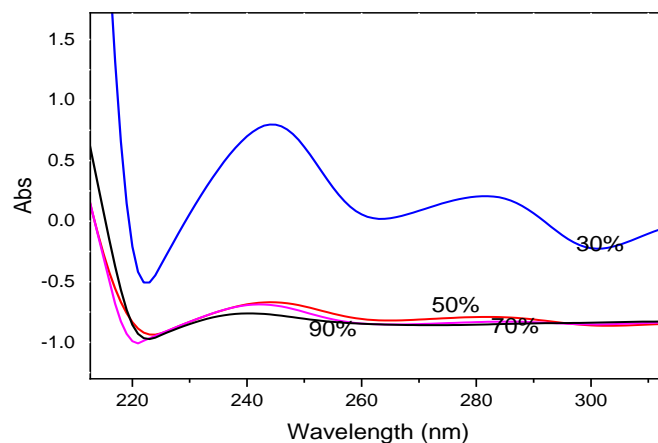


Fig. 19: UV-visible Spectra of Erdosteine in different mole fraction of ethanol-water mixed solvent (0, 30, 50, 70, 90%, Vol %) after time 72 hr.

From Figures (17, 18, and 19) and Table 12, It was found that there are slightly shift in wavelength (λ) as the time intervals and as the mole fraction of ethanol increased. On the other hand, it was found that the absorbance of Erdosteine decrease as the percentage of ethanol increase (Figure 20). This may be due to the

distributions in the hydrogen bonding in solution, where hydrogen bonding breaking between ethanol-ethanol molecules, and hydrogen bond forming between ethanol-Erdosteine

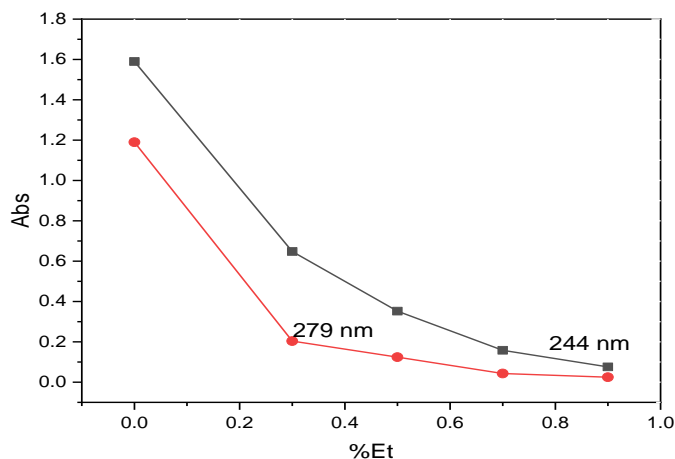


Fig. 20: Effect of ethanol percentage on the absorbance of UV-visible Spectra of Erdosteine

3.5.2-Effect of time on the conductivity and pH:

In studying the effect of time on the solvation of Erdosteine in water solvent at 298°K, from the measurements of the electrolytic conductivity and the pH at different time intervals, it was found that pH and

Table13: The effect of time (hr) and ethanol % on the conductivity($\mu\text{s}/\text{cm}$) and pH values of Erdosteine in ethanol-water mixed solvents at 298 K⁰

conductivity decrease as the time and the ethanol % increase, as data in Table 13. The conductivity decrease as ethanol % increase may be as a result of low dielectric constant of ethanol than water.

Time	Ethanol Vol.%	pH	Conductivity, ($\mu\text{s}/\text{cm}$)
00:00	zero%	7.44	188
	30 %	7.49	73
	50 %	7.45	33
	70 %	7.63	14
	90 %	9.67	5
24:00	zero%	7.50	180
	30 %	7.53	69
	50 %	7.57	32
	70 %	7.31	14
	90 %	8.82	4
48:00	zero%	6.42	175
	30 %	6.77	72
	50 %	6.81	33
	70 %	6.60	15
	90 %	7.80	4
72:00	zero%	5.35	170
	30 %	6.37	75
	50 %	6.06	34
	70 %	5.97	18
	90 %	6.83	5

3.5.3- Refractive index, atomic polarization, molar refraction and polarizability:

The refractive index of a liquid can be measured with the help of an instrument called Abbe

Refract meter. A thin film of the liquid is placed between the two prisms. Light from a sodium lamp is made to fall on lower side of the lower prism with the help of a mirror. The hypotenuse surface of the lower prism is ground and, therefore, light enters the liquid

at all angles of incidence. However, no ray can enter the upper prism with greater angle of refraction than the grazing incidence (i.e., at an angle) slightly less than 90°C. Thus the view in the telescope appears to be divided into two bands, one bright and one dark. The prism assembly is rotated with the help of a side knob till the cross wire of the telescope coincides with the edge of the bright band. A pointer attached to the prism assembly indicates the refractive index on the scale calibrated to read refractive indices directly.

The refractive index measurements had been used to study the solvation of some substances in different solutions like solvation properties of Glycyl-Glycine and Glycyl-L-leucine in aqueous acetate solutions which show that the interactions between ions of acetate salt and the charged end and/or peptide groups become stronger with increasing concentrations of the co solutes. A similar trend was found for diglycine in aqueous KCl, NaA and MgA [56].

The refractive indices and the solvent-solvent interaction processes depend on the nature of the solvent and on its physical properties such as the dielectric constant, the dipole moment and the donor number. The refractive indices can be obtained from the measured values of the refractive indices [57]. The refractive indices, of Erdosteine in ethanol-water mixed solvents at 298 K° are represented in Table 14. From the measured values of the refractive indices, the atomic polar, the molar refraction and the polarizability were calculated [58-59] and represented

Table 14: Refractive indices (n_D), the atomic polar (P_A), the molar refraction (R_m) and the polarizability (α) of Erdosteine in ethanol-water mixed solvents at 298 K°

Mole fraction of ethanol (x_1) by wt.	n_D	P_A	R_m (cm ³ /mol)	$\alpha \times 10^{-23}$ (cm ³)
0.0000	1.364	1.9535	54.310	2.1534
0.0331	1.365	1.9563	54.829	2.1740
0.0715	1.364	1.9546	55.403	2.1967
0.1166	1.363	1.9500	55.294	2.1925
0.1704	1.362	1.9477	55.240	2.1903
0.2355	1.359	1.9417	55.006	2.1810
0.3161	1.355	1.9283	54.909	2.1772
0.4182	1.350	1.9150	55.372	2.1955
0.5520	1.346	1.9014	55.257	2.1910
0.7349	1.345	1.8991	56.314	2.2329

3.5.4- Density measurements and Molal Volume Calculations:

The solvation process can be studied also using the density measurements and the molal volume calculations. The density of Erdosteine in ethanol-water mixed solvents at 298 K° was measured experimentally and represented in Table 15. From the

in Table 14.

Also from the values of the measured refractive indices of Erdosteine with different alcohol mole fractions, the molar refraction (R_m) can be calculated [60]

$$R_m = \frac{n^2 - 1}{n^2 + 2} \rho V = PA + PE = PD + PT \quad (11)$$

Where $V\phi$ is the apparent molar volume of the surfactant in solution, n is the refractive index of the surfactant solution. The right-hand side of **equation (11)** is equal to the total molar polarization or the distortion polarization which equal to the summation of both the electron polarization (PE) and the atomic polarization (PA). The atomic polarization (PA) was calculated [61] from the following equation

$$PA = \frac{1}{3} \epsilon_0 N \alpha^2 \quad (12)$$

The mean value of the molecular dipole polarizability (α ; dipole moment induced by electric field) can be calculated from the optical refractive index (n) of a material containing N molecules per unit volume.

Where $n^2 = N / -V$, N is the Avogadro's number and (ϕV) is the apparent molar volume.

measured density, the solvated radius (r), the molal volume (V_Q), the Wander Walls volume (V_w) and the electrostriction volume (V_e) of Erdosteine in ethanol-water mixed solvents at 298 K° were calculated [62-64] and represented in Table 15.

From the molar concentration and the density values, the apparent molal volumes, $V\phi$ of Erdosteine

in ethanol-water mixed solvents, at 298.15 K, were calculated using the following equation (13)

$$V\phi = M/\rho - 1000/m(1/\rho^0 - 1/\rho) \quad (13)$$

Where M is the molecular weight of Erdosteine, m is the molal concentration of Erdosteine and in solution, ρ and ρ^0 are the densities of solution and solvent, respectively. The calculated apparent molal volumes, $V\phi$ of Erdosteine in ethanol-water mixed solvents at 298 K^o, are given in Table 15.

The packing density is the relation between the Van der Waals volume and the molal volume of relatively large molecules is found to be constant [65-66]. Therefore, it is possible to calculate the Van der Waals volumes (V_w) of Erdosteine under study by

apply the following equation (14).

$$\text{Packing density (P)} = V_w / V\phi = 0.661 \quad (14)$$

The electrostriction volume (V_e) which is the volume compressed by the solvent [65-68], can be calculated using the following equation.

$$V_e = V_w - V\phi \quad (15)$$

The values of the solvated radius, Van Der Waal volume and the electrostriction volume are reported in Table 15.

Inspection of the data in Table 15, we can note that, as the mole fraction of ethanol increase the density decrease and the volume increase, this may be related to the low density of pure ethanol than that of water.

Table 15: The density (ρ), the solvated radius (r), the molal volume (V_Q), the Wander Walls volume (V_w) and the electrostriction volume (V_e) of Erdosteine in ethanol-water mixed solvents at 298 K^o

Mole fraction of ethanol (x_1) by wt.	ρ g/cm ³	V_Q (cm ³ /mol)	r (cm)	V_w (cm ³ /mol)	V_e (cm ³ /mol)
0.0000	1.232	243.655	3.875	161.056	-82.599
0.0331	1.016	245.381	3.884	162.197	-83.184
0.0715	1.004	248.314	3.899	164.135	-84.178
0.1166	1.002	248.809	3.902	164.462	-84.346
0.1704	1.001	249.055	3.903	164.625	-84.429
0.2355	1.000	249.301	3.905	164.788	-84.513
0.3161	0.990	251.817	3.918	166.451	-85.366
0.4182	0.970	257.008	3.944	169.882	-87.126
0.5520	0.960	259.684	3.958	171.651	-88.032
0.7349	0.940	265.207	3.986	175.302	-89.905

4. Conclusions

The Erdosteine drug acts as good and efficient corrosion inhibitor for the corrosion of 304L SS in 1M HCl solution. The IE decreases with rise of temperature, but increases with increasing the dose of the drug. The inhibition of 304L SS corrosion by Erdosteine can be attributed to the adsorption ability of drug molecules onto the reactive sites of the metal surface. The adsorption of the drug on 304L SS obeys Langmuir adsorption isotherm. Polarization data indicate that the drug acts as a mixed-type inhibitor. AFM reveals the formation of a smooth uniform surface on 304L SS in the presence of the drug that indicates the formation of a good protective layer on the metal surface. The results obtained from different measurements gave consistent results.

ACKNOWLEDGEMENTS

All our gratitude to the anonymous referees for their careful reading of the manuscript and valuable comments which helped in shaping this paper to the

present form. We thank all laboratory staff of corrosion chemistry from the University of Mansoura and Port Said (Egypt) for their kind cooperation.

References

- [1] Bin C, Shen. Corrosion Inhibition of 304L Stainless Steel by Dicyclohexyl Thiourea in HCl Solution, in: Adv Mater Res, Trans Tech Publ. 239 (2011) 1901–1906.
- [2] Elayyachy M, Hammouti B, El Idrissi A, New telechelic compounds as corrosion inhibitors for steel in 1 M HCl, Appl Surf Sci. 249 (2005) 176–182.
- [3] Eghbali F, Moayed MH, Davoodi A, Ebrahimi N, Critical pitting temperature (CPT) assessment of 2205 duplex stainless steel in 0.1 M NaCl at various molybdate concentrations, Corros Sci. 53 (2011) 513–522.
- [4] Abdallah M, Rhodanine azosulpha drugs as corrosion inhibitors for corrosion of 304 stainless

- steel in hydrochloric acid solution, *Corros Sci.* 44 (2002) 717–728.
- [5] Fouda AS, Ellithy AS, Inhibition effect of 4-phenylthiazole derivatives on corrosion of 304L stainless steel in HCl solution, *Corros Sci.* 51 (2009) 868–875.
- [6] Jafari H, Sayin K, Electrochemical and theoretical studies of adsorption and corrosion inhibition of aniline violet compound on carbon steel in acidic solution, *J Taiwan Inst Chem Eng.* 56 (2015) 181–190.
- [7] Ramya K, Josephv A, Synergistic effects and hydrogen bonded interaction of alkyl benzimidazoles and thiourea pair on mild steel in hydrochloric acid, *J Taiwan Inst Chem. Eng.* 52 (2015) 127–139.
- [8] Adawy AI, Abbas MA, Zakaria K, New Schiff base cationic surfactants as corrosion inhibitors for carbon steel in acidic medium: weight loss, electrochemical and SEM characterization techniques, *Res Chem Intermed.* 42 (2016) 3385–3411.
- [9] Deyab MA, Keera ST, El Sabagh SM, Chlorhexidine digluconate as corrosion inhibitor for carbon steel dissolution in emulsified diesel fuel, *Corros Sci.* 53 (2011) 2592–2597.
- [10] Deyab MA, Adsorption and inhibition effect of Ascorbyl palmitate on corrosion of carbon steel in ethanol blended gasoline containing water as a contaminant, *Corros Sci.* 80 (2014) 359–365.
- [11] Fouda AS, Elmorsi MA, Fayed TA, Hassan AF, Soltan M, Corrosion inhibitors based on antibiotic derivatives for protection of carbon steel corrosion in hydrochloric acid solutions, *Int J Adv Res.* 2 (2014) 788–807.
- [12] Fouda AS, Ibrahim H, Rashwaan S, El-Hossiany A, Ahmed RM, Expired drug (pantoprazole sodium) as a corrosion inhibitor for high carbon steel in hydrochloric acid solution, *Int J Electrochem Sci.* 13 (2018) 6327–6346. doi : 10.20964/2018.07.33.
- [13] Samide A, Tutunaru B, Negrila C, Corrosion inhibition of carbon steel in hydrochloric acid solution using a sulfa drug, *Chem Biochem Eng. Q.* 25 (2011) 299–308.
- [14] Fouda AS, Rashwan SM, Abdelfatah M, Corrosion inhibition of stainless steel 304 in hydrochloric acid solution using clindamycin antibiotic as eco-friendly inhibitor, *Zaštita Mater.* 60 (2019) 3–17.
- [15] Mollaamin F, Kandemirli F, Monajjemi M, Analysis of Pyridine, Picoline and Lutidine's Adsorption Behavior on The Al (111)-lattice, Biointerface research in applied chemistry 12(3) (2022) 3225-3237.
- [16] Solmaz R, Kardaş G, Erbil M, The Rhodanine inhibition effect on the corrosion of a mild steel in acid along the exposure time, *Prot Met.* 43 (2007) 476–482.
- [17] Fouda AS, El-Wakeel AM, Shalabi K, El-Hossiany A, Corrosion inhibition for carbon steel by levofloxacin drug in acidic medium, *Elixir Corros Day.* 83 (2015) 33086–33094.
- [18] Abdallah M, Zaaferany I, Al-Fahemi JH, Abdallah Y, Fouda AS, Antibacterial cephalosporin as inhibitors for the corrosion of iron in hydrochloric acid solutions, *Int J Electrochem Sci.* 7 (2012) 6622–6637.
- [19] Zhang DQ, Cai QR, He XM, Gao LX, Kim GS, Corrosion inhibition and adsorption behavior of methionine on copper in HCl and synergistic effect of zinc ions, *Mater Chem Phys.* 114 (2009) 612–617.
- [20] Oguzie EE, Corrosion inhibition of mild steel in hydrochloric acid solution by methylene blue dye, *Mater Lett.* 59 (2005) 1076–1079.
- [21] Abdallah M, Fouda AS, El-Ashrey SM, Corrosion inhibiting properties of some crown ethers on corrosion of stainless steel (types 304 and 316) in hydrochloric acid, *Zaštita Mater.* 49 (2008) 9–22.
- [22] Morad MS, Inhibition of iron corrosion in acid solutions by Cefatrexyl: Behaviour near and at the corrosion potential, *Corros Sci.* 50 (2008) 436–448.
- [23] Eddy NO, Odoemelam SA, Ekwumemgbo P, Inhibition of the corrosion of mild steel in H₂SO₄ by penicillin G, *Sci Res Essays.* 4 (2009) 33–38.
- [24] Eddy NO, Odoemelam SA, Inhibition of the corrosion of mild steel in acidic medium by penicillin V potassium, *Adv Nat Appl Sci.* 2 (2008) 225–232.
- [25] Singh AK, Quraishi MA, Effect of Cefazolin on the corrosion of mild steel in HCl solution, *Corros Sci.* 52 (2010) 152–160. doi : 10.1016/j.corsci.2009.08.050.
- [26] Shukla SK, Quraishi MA, Ceftriaxone: a novel corrosion inhibitor for mild steel in hydrochloric acid, *J Appl Electrochem.* 39 (2009) 1517–1523.
- [27] Abdallah M, Alfakeer M, Alonazi AM, and Al-Juaid SS, Ketamine drug as an inhibitor for the corrosion of 316 stainless steel in 2M HCl solution. *Int. J. Electrochem. Sci.* 14(2019) 10227-10247.
- [28] Abdel Hameed R, Essa A, Mohamed D, Abdallah M, Aljohani M, Al-Mhyawi S, Soluman M, and Arafa EI, Evaluation of Expired Augmentine Drugs as Corrosion Inhiitor for Carbon Steel Alloy in 1.0 n hcl Acidic Environment Using Analytical Techniques. *Egyptian Journal of Chemistry,* 65(4) (2022) 1-2.
- [29] Abdel Hameed RS, Qureshi MT, Mohamed D, Abdallah M, Aljuhani EH, Aljohani MM, Soliman MS, and Al-Mhyawi SR, Recycling and application of expired desloratadine medicinal

- drugs for inhibition of steel corrosion in acid environment: Analytical studies *Int. J. Corros. Scale Inhib.* 10(3) (2021) 1748–1765
- [30] Abdallah M, Fawzy A, and Bahir AA, Expired amoxicillin and cefuroxime drugs as efficient anticorrosives for Sabic iron in 1.0 M hydrochloric acid solution. *Chemical Engineering Communications*, (2020) 1-28.
- [31] Mohanty KC , Thiappanna G , Singh V, Mancini C, Evaluation of efficacy and safety of unused Erdosteine in patients affected by exacerbation of chronic bronchitis and receiving ciprofloxacin as basic treatment, *J Clin Res.* 4 (2001) 35–39.
- [32] Fouda AS , Abd El-Maksoud SA , El-Hossiany A , Ibrahim A , Evolution of the corrosion-inhibiting efficiency of novel hydrazine derivatives against corrosion of stainless steel 201 in acidic medium, *Int J Electrochem. Sci.* 14 (2019) 6045–6064.
- [33] Fouda AS, Rashwan S, El-Hossiany A , No Title, *JCBPS.* 19(1) (2018) 001.
- [34] El Achouri M , Kertit S , Gouttaya HM , Nciri B, Bensouda Y, Perez L , Infante MR , Elkacemi K , Corrosion inhibition of iron in 1 M HCl by some gemini surfactants in the series of alkanediyl- α , ω -bis-(dimethyl tetradecyl ammonium bromide), *Prog Org Coatings.* 43 (2001) 267–273.
- [35] Fouda AS , Abd El-Maksoud SA , Belal AAM , El-Hossiany A , Ibrahim A , Effectiveness of some organic compounds as corrosion inhibitors for stainless steel 201 in 1M HCl: experimental and theoretical studies, *Int J Electrochem Sci.* 13 (2018) 9826–9846.
- [36] Mertens SF, Xhoffer C, De Cooman BC, Temmerman E, Short-term deterioration of polymer-coated 55% Al-Zn—part 1: behavior of thin polymer films, *Corrosion.* 53 (1997) 381–388.
- [37] Fouda AS , El-Ghaffar MAA , Sherif MH , El-Habab AT, El-Hossiany A , Novel Anionic 4-Tert-Octyl Phenol Ethoxylate Phosphate Surfactant as Corrosion Inhibitor for C-steel in Acidic Media, *Prot Met Phys Chem Surfaces.* 56 (2020) 189–201. doi : 10.1134/S2070205120010086.
- [38] Fouda AS, Abdel Azeem M, Mohamed SA, No Title, *Int. J. Electrochem Sci.* 14 3932. 14 (2019) 3932.
- [39] Fouda AS , Abdel-Latif E , Helal HM , El-Hossiany A , Synthesis and Characterization of Some Novel Thiazole Derivatives and Their Applications as Corrosion Inhibitors for Zinc in 1 M Hydrochloric Acid Solution, *Russ J Electrochem.* 57 (2021) 159–171. doi: 10.1134/S1023193521020105.
- [40] Fouda AS, Eissa M, El-Hossiany A, Ciprofloxacin as eco-friendly corrosion inhibitor for carbon steel in hydrochloric acid solution, *Int J Electrochem Sci.* 13 (2018) 11096–11112.
- [41] Fouda AS, Motaal SMA, Ahmed AS, Sallam HB, Corrosion Protection of Carbon Steel in 2M HCl Using Aizoon canariense Extract, *Biointerface Res Appl Chem.* 12 (2021) 230–243. doi: 10.33263/briac121.230243.
- [42] Elgyar OA , Ouf AM , El-Hossiany A, Fouda AS , The inhibition action of viscum album extract on the corrosion of carbon steel in hydrochloric acid solution, *Biointerface Res Appl Chem.* 11 (2021) 14344–14358. doi:10.33263/BRIAC116.1434414358.
- [43] Kuş E , Mansfeld F , An evaluation of the electrochemical frequency modulation (EFM) technique, *Corros Sci.* 48 (2006) 965–979.
- [44] Khaled MA , Ismail MA , El-Hossiany A , Fouda AS , Novel pyrimidine-bichalcophene derivatives as corrosion inhibitors for copper in 1 M nitric acid solution, *RSC Adv.* 11 (2021) 25314–25333.
- [45] Fouda AS , Ahmed RE , El-Hossiany A , Chemical, Electrochemical and Quantum Chemical Studies for Famotidine Drug as a Safe Corrosion Inhibitor for α -Brass in HCl Solution, *Prot Met Phys Chem Surfaces.* 57 (2021) 398–411.
- [46] Amar H , Braisaz T, Villemin D , Moreau B , Thiomorpholin-4-ylmethyl-phosphonic acid and morpholin-4-methyl-phosphonic acid as corrosion inhibitors for carbon steel in natural seawater, *Mater Chem Phys.* 110 (2008) 1–6.
- [47] Umoren SA , Solomon MM , Eduok UK , Inhibition of mild steel corrosion in H₂SO₄ solution by coconut coir dust extract obtained from different solvent systems and synergistic effect of iodide ions: ethanol and acetone extracts, *J Environ Chem Eng.* 2 (2014) 1048-1060
- [48] Kalaivani R , Narayanaswamy B, Selvi JA , Amalraj AJ, Jeyasundari J , Rajendran S, Corrosion inhibition by Prussian blue, *Port Electrochim. Acta.* 27 (2009) 177–187. doi: 10.4152/pea.200902177.
- [49] Fouda AS , El-Gharkawy ES , Ramadan H , El-Hossiany A , Corrosion resistance of mild steel in hydrochloric acid solutions by clinopodium actions as a green inhibitor, *Biointerface Res Appl Chem.* 11 (2021) 9786–9803.
- [50] Karthikeyan S , Kumar H , Inhibition of mild steel corrosion in hydrochloric acid solution by cloxacillin drug, *J Mater Environ Sci.* 3(5) (2012) 925-934.
- [51] Fouda AS , Badr SE , Ahmed AM , El-Hossiany A , Chemical and electrochemical corrosion of a copper alloy in aqueous solutions by using morus alba extract as an eco-friendly inhibitor, *Int J*

- Corros Scale Inhib. 10 (2021) 1011–1029. doi: 10.17675/2305-6894-2021-10-3-12.
- [52] Damaskin BB, Petrii OA, Batrakov B, Adsorption of Organic Compounds on Electrodes; Plenum Press: New York, 1971.
- [53] El-Dossoki FI, Abou El-Hasan EE, Abdelrhman EG, Solvation of Parachloro Meta Xylenol (PCMX) in Alcohols-Aqueous Solutions at 293.15 K. International Journal of Advanced Research in Chemical Science (IJARCS). 3 (19) (2016) pp19-28.
- [54] El-Dossoki FI, El-Damarany MM, Solvation of basic and neutral amino Acids in aqueous electrolytic solutions, measurements and modeling, J Chem Eng Data, 60 (10) (2015) :2989.
- [55] El-Dossoki FI, The Effect of 18-crown-6 on the solubility and thermodynamic parameters of Li₂CO₃, Na₂CO₃, NaCl, CH₃COONa and KCl in methanol and ethanol, Indian J Chem. A, 44 (2005) 1594-1596.
- [56] El-Dossoki FI, 'Volumetric and solvation properties of glycyl- glycine and glycyl-l-leucine in aqueous acetate solutions', Journal of Solution Chemistry, 44(2) (2015), 264–279. doi: 10.1007/s10953-015-0314-4.
- [57] El-Dossoki FI, 'Refractive Index and Density Measurements for Selected Binary Protic-Protic, Aprotic-Aprotic, and Aprotic- Protic Systems at temperatures from 298.15 K to 308.15 K', Journal of the Chinese Chemical Society, 54(1) (2007), 1129–1137. doi: 10.1002/jccs.200700162.
- [58] El-Dossoki FI, Gomaa EA, Abdelzاهر MA, Micellization, Molal Volume and Polarizability of Benzyl and Allyl-Methyl Imidazolium Ionic Liquids in Aqueous and Alcoholic-Aqueous Solvents, Iranian Chemical Society, (2021). doi : 10.1007/s13738-021-02336-3
- [59] El-Dossoki FI, Abd El-Maksoud SA, Migahed MA, Gouda MM, Micellization and Solvation Properties of Newly Synthesized Imidazolium- and Aminium- Based Surfactants, ACS Omega, 5 (16) (2020) 9429–9441. doi : 10.1021/acsomega.0c00603
- [60] El-Harakany AA, El-Dessouky M, Taha AA, Bassiony AF, Solubilities and thermodynamic functions of transfer of substituted benzoic acids and aliphatic amine derivatives from water to water- sulpholane mixtures at different temperatures, Egyptian Journal of Chemistry, 45(1) (2002), 1–32.
- [61] Mognaschi E, Laboranti LM, 'Association of pure polar liquids: dielectric properties of docosanoic acid', Journal of Chemical Society, Faraday Transactions, 92(18) (1996), 3367–3369.
- [62] El-Dossoki FI, Fahmy A, Mohamed T, Abu-Saied M, Helaly H, Novel PVA/Methoxytrimethylsilane elastic composite membranes: preparation, characterization and DFT computation, Journal of Molecular Structure 1235 (2021) 130173, doi : 10.1016/j.molstruc.2021.130173
- [63] El-Dossoki FI, Gomaa EA, Hamza OK, Solvation Thermodynamic Parameters for Alkyl Benzyl Dimethyl Ammonium Chloride and Cetyl Trimethyl Ammonium Chloride Surfactants in Water and Alcoholic -Water Solvents JCED, 64 (10) (2019) 4482-4492. doi: 10.1021/acs.jced.9b00527
- [64] El-Dossoki FI, Phase Diagrams, Molal Volumes and Polarizabilities of (Lysine, Methionine Amino Acids- Alcohol-Water) Tri-Component Systems. International Research Journal of Pure & Applied Chemistry (IRJPAC), 16(2) (2018) 1-11. doi: 10.9734/IRJPAC/2018/40184.
- [65] Millero F, Apparent molal expansibilities of some divalent chlorides in aqueous solution at 25.deg, Journal of Physical Chemistry, 72(13) (1968), 4589–4593.
- [66] King E, Volume changes for ionization of formic, acetic, and butyric acids and the glycinium ion in aqueous solution at 25.deg, Journal of Physical Chemistry, 73(5) (1969), 1220–1232.
- [67] Millero J, Surdo A, Shin C, The apparent molal volumes and adiabatic compressibility of aqueous amino acids at 25 C, J Phys Chem, 82(7) (1978), 784–792.
- [68] Gopal R, Siddiqi M, Study of ion-solvent interaction of some tetraalkyl ammonium and common ions in N-methylacetamide from apparent molal volume data, The Journal of Physical Chemistry, 73(10) (1969), 3390–3394.